Available online at www.sciencedirect.com

ScienceDirect

Geochimica et Cosmochimica Acta 317 (2022) 218–233

Geochimica et Cosmochimica Acta

www.elsevier.com/locate/gca

Iron and manganese shuttle has no effect on sedimentary thallium and vanadium isotope signatures in Black Sea sediments

Xinming Chen [a,*], Siqi Li [a], Sean M. Newby [a], Timothy W. Lyons [b], Fei Wu [c], Jeremy D. Owens [a]

[a] *Department of Earth, Ocean, and Atmospheric Science and National High Magnetic Field Laboratory, Florida State University, Tallahassee, FL, USA*

[b] *Department of Earth Sciences, University of California, Riverside, CA, USA*

[c] *School of Earth Sciences, State Key Laboratory of Geological Processes and Mineral Resources, China University of Geosciences, Wuhan 430074, China*

Received 1 June 2021; accepted in revised form 6 November 2021; available online 12 November 2021

Abstract

Thallium and V isotopes in organic-rich sediments have recently been explored for reconstructing marine oxygenation by tracking the burial of Mn oxides either locally or globally. The 'Fe and Mn shuttle' is a well known mechanism that can transport elements associated with Fe and Mn oxide phases formed under mildly oxidizing shallow water environments both laterally and vertically to euxinic (sulfidic water column) deep waters. The Fe and Mn shuttle has been demonstrated to strongly affect Fe and Mo isotope compositions of sediments accumulating beneath anoxic and euxinic settings. Similar to Mo, Tl and V are also enriched in oceanic ferromanganese crust and nodules, which impart the largest isotopic offsets from modern seawater for Tl and V. Thus, the mechanism of an Fe and Mn shuttle has the potential to, but currently unconstrained, affect Tl and V isotopic compositions (ε^{205}Tl and δ^{51}V) in organic-rich sediments in the modern and ancient records.

We have used Black Sea sediments that are known to preserve enrichment and sedimentary isotope signatures for an Fe shuttle. This is due to an Fe transport from the more oxic margin to the deep euxinic basin and corresponding enrichment in the underlying sediments. These samples were used to test for a potential Fe and Mn shuttle effect on ε^{205}Tl and δ^{51}V in sediments deposited under oxic, suboxic, and euxinic water columns. Authigenic ε^{205}Tl from all three depositional settings is indistinguishable (-2.7 ± 0.3, -2.4 ± 0.5, and -2.4 ± 0.3), which is within error of the Black Sea surface seawater (-2.2 ± 0.3). In contrast, oxic and suboxic sediment have similar δ^{51}V values (-1.06 ± 0.33‰ and -1.04 ± 0.30‰), which are significantly more negative than euxinic sediments (-0.57 ± 0.06‰).

All the sediments deposited under oxic, suboxic, and euxinic water columns in the Black Sea capture ε^{205}Tl of the surface seawater because there is almost no permanent burial of Mn oxides in this basin. This finding is consistent with the indistinguishable ε^{205}Tl between the surface seawater and the riverine input. Sedimentary δ^{51}V appears to be controlled predominantly by the redox state of the depositional environments with little effect from an Fe or Mn shuttle. The lack of Fe and Mn shuttle effect on ε^{205}Tl and δ^{51}V in the Black Sea is likely due to the shallow (~100 m) chemocline in the strongly, 2000-m deep redox-stratified water column of this basin and very slow deep-water renewal rate. Iron and Mn in oxides are not delivered to the sediments, instead, they are dissolved and captured in the water column as iron sulfide and reduced

* Corresponding author.
E-mail address: xchen6@fsu.edu (X. Chen).

https://doi.org/10.1016/j.gca.2021.11.010

Mn mineral phases. Our results suggest that Fe and Mn shuttle transport mechanisms may not strongly affect Tl and V isotopes, at least in extreme cases of water column redox stratification. Further work is required to constrain the isotopic signals using other modern and, by inference, diverse ancient settings for additional shuttling mechanisms.

Keywords: Tl isotopes; V isotopes; Suboxic; Reducing; Euxinic

1. INTRODUCTION

The Neoproterozoic rise of atmospheric oxygen coincides with the appearance of first early animals, suggesting a cause-and-effect relationship, however, the details and veracity of this conclusion are still debated (e.g., Cole et al., 2020; Knoll and Sperling, 2014; Mills and Canfield, 2014; Raman et al., 2013; Reinhard et al., 2016; Sperling et al., 2013). To unravel any causal relationship between oxygenation and the evolution of animals, it is critical to track low but non-zero bottom water oxygen concentrations (2–20 μM), which have been suggested as the minimum range required for animals (e.g., Xiao, 2013). Variations of thallium ($^{205}Tl/^{203}Tl$) and vanadium ($^{51}V/^{50}V$) isotope ratios in organic-rich sediments are being explored to fingerprint low but non-zero bottom water oxygen concentrations in the oceans—specifically as reflected in the burial of Mn oxides (Nielsen et al., 2009a; Nielsen et al., 2011a; Nielsen et al., 2017; Ostrander et al., 2017; Owens et al., 2017; Them et al., 2018; Bowman et al., 2019; Ostrander et al., 2019a; Owens, 2019; Wu et al., 2019b; Fan et al., 2020; Nielsen, 2020). The strength of these novel proxies, however, lies with our understanding of the factors that control variations of Tl and V isotope signals in organic-rich sediments in modern marine conditions.

Variations of Tl and V isotope compositions in seawater are governed by changes in the integrated redox state of the oceans where these two trace metals are scavenged from seawater by oxic (e.g., pelagic), anoxic, and euxinic sediments with varying isotope fractionations (Emerson and Huested, 1991; Rehkämper et al., 2002; Rehkämper and Nielsen, 2004; Nielsen et al., 2009a; Nielsen et al., 2011a; Nielsen et al., 2017; Owens et al., 2017; Wu et al., 2019b; Wu et al., 2020; Nielsen, 2020). For Tl, organic-rich sediments deposited under anoxic and euxinic (sulfidic) bottom water columns tend to capture the seawater isotopic composition (e.g., Tl isotope compositions in euxinic sediments (–2.3 ± 0.3) in the Black Sea are similar to the oxic surface water values (–2.2 ± 0.3), within error). In contrast, oxic sediments (specifically associated with the Mn oxide mineral birnessite) cause the largest isotope fractionation offset from seawater value of +12 to +18, with ^{205}Tl preferentially buried (Rehkämper et al., 2002; Nielsen et al., 2009a; Nielsen et al., 2011a; Peacock and Moon, 2012; Nielsen et al., 2017; Owens et al., 2017). Sedimentary authigenic V isotope compositions in oxic, anoxic, and euxinic sediments are 1.1 ± 0.3‰, 0.7 ± 0.2‰, and 0.4 ± 0.2‰ lighter than that of modern seawater (0.20 ± 0.07‰, 2 SE), respectively, and thus strongly depend on the local redox state of the depositional environment (Schuth et al., 2019; Wu et al., 2019a, 2019b; Wu et al., 2020; Nielsen, 2020). Both isotopic systems show the largest isotope fractionation in oxic sediments associated with oxide phases (Mn only for Tl and likely both Fe and Mn for V) and the smallest, if any, isotopic offsets in euxinic sediments. Both Tl and V concentrations and isotopes have a conservative profile in the modern ocean as neither have significant bioutilization (Millero, 2013) and have long modern marine residence times (~20 kyr and ~90 kyr, respectively) compared to ocean mixing time (~1 kyr) (Owens, 2019; Nielsen, 2020; Jenkins, 2003). As a result, authigenic Tl and V isotope compositions in euxinic sediments can reflect variations of seawater isotopic signals due to changes in redox conditions of oceans through time, particularly as related to burial of Fe and/or Mn oxides (Nielsen et al., 2017; Owens et al., 2017; Wu et al., 2020).

Beyond the redox state of the depositional environment, Fe and Mn shuttles have been demonstrated to significantly enhance the authigenic accumulation of trace metals (e.g., Fe, Mn, and Mo) via two different pathways (Little et al., 2015). One is the formation of Fe and Mn oxide particles in an oxic water column and subsequent quantitative delivery of their sorbed trace metals (e.g., Mo, V, and Ni) directly to sediment due to the redox boundary at or near the sediment–water interface (Little et al., 2015). This pathway has been termed the 'particulate shuttle', which has been used to interpret strong sedimentary enrichments of Mo in modern anoxic basins such as the weakly restricted Baltic Sea (Scholz et al., 2013). The other has been termed the 'benthic Fe and Mn redox shuttle', which involves the transportation of solid-phase Fe and Mn oxides from the oxic shelf with suboxic sediments to the deep euxinic basin, where they react with free sulfide and precipitate as MnS_2/rhodochrosite and FeS/Fe_3S_4/pyrite (Lyons and Severmann, 2006; Lewis and Landing, 1991; Little et al., 2015; Anderson and Raiswell, 2004; Lyons, 1997). This type of shuttle was proposed to result in the large-scale lateral shuttling of Fe and Mn to the deep euxinic basin of the Black Sea, elevating Fe/Al and Mn/Al ratios in the euxinic sediments of this basin (Lewis and Landing, 1991; Raiswell and Anderson, 2005; Lyons and Severmann, 2006; Lenstra et al., 2019, 2020).

Because of the significant shuttling effects on trace metal enrichments in sediments, Fe and Mn shuttles can also shift the isotopic compositions toward values lighter than contemporaneous seawater (e.g., for $\delta^{98}Mo$ and $\delta^{56}Fe$) in anoxic and euxinic sediments in modern redox-stratified basins (e.g., Cariaco Basin and Baltic Sea), and similar effects have been observed in oxygen minimum zones along upwelling continental margin systems (e.g., Peru margin) (Lyons and Severmann, 2006; Severmann et al., 2008; Algeo and Tribovillard, 2009; Dellwig et al., 2010; Scholz

et al., 2011, 2013, 2014, 2017; Noordmann et al., 2015; Kendall et al., 2017; Lenstra et al., 2019; Brüske et al., 2020; Lenstra et al., 2020). The effect of Fe and Mn shuttling on authigenic Mo isotope signals has also been implicated in organic-rich black shales in deep time (Herrmann et al., 2012; Kurzweil et al., 2016; Ostrander et al., 2019b). This shuttling results from the strong affinity of Mo to Fe-Mn oxides. Further uptake is associated with crusts and nodules, with extremely high Mo concentrations (~400 ppm) under modern oxic seawater conditions (dissolved Mo concentration ~10 ppb) and the largest observed isotope fractionation (up to 3‰) during Mo adsorption to these oxides (Barling et al., 2001; McManus et al., 2002; Siebert et al., 2003; Anbar, 2004; Barling and Anbar, 2004; McManus et al., 2006; Poulson et al., 2006; Siebert et al., 2006; Neubert et al., 2008; Wasylenki et al., 2008; Goldberg et al., 2009; Nägler et al., 2011; Wasylenki et al., 2011; Hein and Koschinsky, 2013; Noordmann et al., 2015; Kendall et al., 2017; Bura-Nakić et al., 2018; Tanaka et al., 2018).

Similar to Mo, Tl and V are also enriched in oceanic Fe-Mn crusts and nodules (~97 ppm and ~639 ppm) relative to dissolved Tl and V concentrations of ~10 ppt and ~2 ppb, respectively. The Fe-Mn crusts and nodules also show the largest isotope fractionations (from +12 to +18 ε -units for Tl and –1.25 ± 0.16‰ for V) in the modern oceans (Rehkämper et al., 2002; Peacock and Moon, 2012; Hein and Koschinsky, 2013; Nielsen et al., 2013; Nielsen et al., 2017; Wu et al., 2019b). Based on these similarities and the strong correlations of V with Fe and Mn oxides in sinking particles of modern redox-stratified basins and oxygen minimum zones (Yigiterhan et al., 2011; Nielsen et al., 2013; Bauer et al., 2017; Scholz et al., 2017), we hypothesize that Fe and Mn shuttles could also affect authigenic Tl and V isotope compositions ($\varepsilon^{205}Tl_{auth}$ and $\delta^{51}V_{auth}$) in anoxic and euxinic sediments. The result would be heavier $\varepsilon^{205}Tl_{auth}$ but lighter $\delta^{51}V_{auth}$ in these sediments relative to sediment deposited under similar redox conditions but without the effect of the Fe and Mn shuttles.

To test the possible impact of Mn and Fe shuttling, we measured Tl and V isotope compositions in oxic, suboxic, and euxinic (anoxic and sulfidic water-column) sediments in the redox-stratified Black Sea, which is widely used as a natural laboratory for constraining modern euxinic systems as a potential analog for ancient settings. The euxinic sediments in this deep basin show significantly elevated Fe/Al and Mn/Al ratios, as well as lighter authigenic Fe and Mo isotope compositions relative to sediments deposited on the oxic shelf, providing strong evidence for large-scale lateral (shelf-to-basin) shuttling of Fe and Mn (the 'benthic Fe and Mn redox shuttle'; Spencer and Brewer, 1971; Lewis and Landing, 1991; Wijsman et al., 2001; Raiswell and Anderson, 2005; Lyons and Severmann, 2006; Severmann et al., 2008; Pakhomova et al., 2009; Eckert et al., 2013; Lenstra et al., 2019; Lenstra et al., 2020). Here, we explore the possible consequences of Fe and Mn shuttling on authigenic Tl and V isotopic signals in Black Sea sediments.

2. SAMPLES

The samples analyzed in this study were collected during the 1988 *R/V Knorr* Black Sea cruise (Fig. 1). The Black Sea is the largest permanently euxinic basin in the modern ocean with a renewal time of ~400–2000 years for the deep-water (Algeo and Lyons, 2006). The O_2/H_2S interface (chemocline) is presently located at ~120–150 m, overlying euxinia (up to ~400–600 μM of total dissolved hydrogen sulfide) that extends to the seafloor at depths > 2000 m in the central basin (Murray, 1989; Rolison et al., 2017).

Detailed descriptions of the sediment cores used here are described elsewhere (Lyons, 1991; Lyons and Berner, 1992; Arthur et al., 1994; Lyons, 1997; Lyons and Severmann, 2006). Briefly, our samples include sediments from the oxic shelf (Station 16, 17, 3, and 4), the chemocline (Station 16B), the shallow euxinic margin (~200 m, Station 5 and 15), and the deep euxinic basin (>2000 m, Station 9 and BC21) (Fig. 1). These sediments were deposited beneath oxic (presence of abundant dissolved oxygen [DO] in water

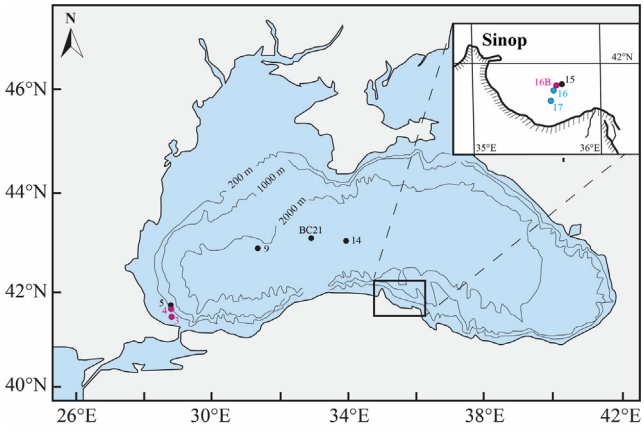

Fig. 1. Geological sampling sites of Black Sea sediments for Tl and V isotope measurements in this study (insert shows the sampling sites 15, 16, 16B, and 17 in the Bay of Sinop region). The blue, pink, and black symbols represent sediments deposited under oxic, suboxic, and euxinic conditions.

with a concentration of 0.5–2.0 ml/L), suboxic [DO concentration of 0–0.5 ml/L and absence of hydrogen sulfide], and euxinic [presence of hydrogen sulfide) bottom waters (Algeo and Li, 2020). The redox states of the local depositional environments for the Black Sea sediments used in this study has been well constrained using iron speciation (Lyons and Severmann, 2006). Specifically, sediments from Station 16 and 17 and the top 4 cm of Station 3 and 4 were deposited under oxygenated bottom waters with organic carbon and calcium carbonate contents averaging at 1.2 ± 0.4 and 20.1 ± 5.3 wt%, respectively (Arthur et al., 1994). Sediments from Station 16B were deposited under suboxic conditions, while Station 3 and 4 (below 4 cm) reflect previous shoaling of the chemocline (Lyons et al., 1993). The average organic carbon and calcium carbonate contents in these sediments were 0.9 ± 0.1 and 18.1 ± 1.8 wt%, respectively. Sediments from Station 5 and 15 were deposited on the euxinic margin (at 198 and 233 m) with mean organic carbon and calcium carbonate contents of 1.7 ± 0.4 and 12.4 ± 1.3 wt%, respectively. Sediments from Station 9 and BC32 deposited in the deep basin (>2000 m) were characterized by high organic carbon contents (5.3 ± 1.0 wt%) and calcium carbonate (52.5 ± 11.3 wt%).

3. METHODS

All sample digestion and elemental purification were completed in a trace metal clean lab at the National High Magnetic Field Laboratory (NHMFL). Acids used in all procedures were double distilled in-house and higher than aristar grade, and the H_2O_2 was aristar grade. All instrumental analyses were performed at the NHMFL.

3.1. Sample preparations

Sedimentary authigenic Tl and V were extracted via hot-leaching and cold-leaching methods, respectively (Wu et al., 2020; Nielsen et al., 2011a). To extract authigenic Tl in sediments, 50–100 mg of powdered samples were mixed with 3 ml of 2 M HNO_3 and heated at 130 °C for 12–15 hours (Nielsen et al., 2011a). The authigenic Tl (soluble fraction) was separated via three cycles of centrifugation at 4000 rpm for 10 minutes. The supernatant from each sample was then digested with 3 ml concentrated HNO_3 + 3 ml concentrated HCl and 3 ml concentrated HNO_3 + 0.2 ml 30% H_2O_2 to break down organic matter. The solutions were completely dried down at 120 °C and then dissolved in 1 M HCl for Tl purification.

In contrast, authigenic V in Black Sea sediments was extracted using the cold-leaching method, which has been demonstrated to be effective in extracting authigenic V with negligible V leached from lithogenic phases (Wu et al., 2020). The authigenic fraction of V was extracted by mixing ~100 mg powdered samples with 3 M HNO_3 at room temperature (~22 °C) for 12–16 hours with constant agitation on a shaker table. The soluble fraction was separated from the insoluble solid via three cycles of centrifugation at 4000 rpm for 10 minutes. The supernatant was pipetted to Teflon vials and digested using 3 ml aqua regia and 3 ml concentrated HNO_3 + 0.2 ml 30% H_2O_2 to remove organic matter. All the solutions were dried down at 120 °C, and then dissolved in 1 ml of 0.8 M HNO_3 for V purification. An aliquot of 40 µl solution from each sample was diluted by 2% HNO_3 for trace element analysis on an Agilent 7500cs quadrupole inductively coupled plasma mass spectrometer (ICP-MS).

3.2. Column chemistry

Thallium was purified using AG1-X8 anion exchange resin following the established protocols (Rehkämper and Halliday, 1999; Owens et al., 2017). About 8–20 hours before Tl purification, 100 µl of brominated H_2O was added to each digested sample. About 100 µl of AG1X8 200–400 mesh resin were loaded to micro-columns. The resin was cleaned using 1.5 ml of 0.1 M HCl-SO_2 solution (5 weight percent of SO_2). The micro-columns were then rinsed with 1.6 ml of 0.1 M HCl. The resin was then conditioned with 1 ml of 0.1 M HCl + 1% brominated water. The samples were loaded into the micro-columns. The resin was then rinsed with 1.8 ml of 0.5 M HNO_3 + 3% brominated water, 1.6 ml of 2.0 M HNO_3 + 3% brominated water, and 1.6 ml of 0.1 M HCl + 1% bromated water to remove matrix in samples. Thallium was eluted from the resin using 1.6 ml of 0.1 M HCl-SO_2 solution. The eluted samples were then dried down completely at 180 °C and digested with 100 µl of aqua regia and 50 µl of concentrated HNO_3 to remove any organics from the column chemistry. The samples were finally dissolved in 0.1 M HNO_3 + 0.1% H_2SO_4. The yield of Tl throughout the column chemistry process was within error of 100%. The amount of Tl from the procedural blank was < 5 pg during Tl purification process.

Vanadium purification was accomplished using two cation- and anion-exchange columns (Wu et al., 2016; Wu et al., 2019b; Nielsen et al., 2011b). Briefly, the first two columns employed cation resin AG50W-X12 (200–400 mesh) to remove Fe, Ti, and other major matrix elements (e.g., Al, Ca, Mn, and Cr). The last two anion-exchange columns used AG1-X8 (200–400 mesh) resin to further remove any matrix (e.g., K and Mg) and isobaric elements (Cr and Ti) remaining in the samples. The eluted solutions from the anion columns were evaporated and digested with aqua regia to remove any organic matter released from the anion resin. The yield of V throughout the V purification process was > 99%. The mass of V from the blank of the V column chemistry is typically less than 2 ng, which is negligible compared to the loaded amount of V (3–5 µg) for our samples.

3.3. Isotope measurements

Thallium isotopes were measured on a Thermo Scientific Neptune multi-collector inductively coupled plasma mass spectrometer (MC-ICP-MS) using an Aridus II desolvating nebulizer for sample introduction. Before isotope analysis, NIST SRM 981 Pb was added to every sample to monitor instrument mass bias. Thallium isotopes were analyzed using the sample-standard bracketing method (Nielsen et al., 2005; Nielsen et al., 2009b; Nielsen et al., 2011b; Nielsen et al., 2017). Thallium isotopic compositions are

Table 1
Summary of elemental contents and Tl and V isotopic compositions in Black Sea sediments deposited under oxic, suboxic, and euxinic water columns.

Station	Depth cm	Depositional setting	Al wt%	Mn ppm	Fe wt%	V ppm	Tl_{auth} ppb	Fe/Al wt%/wt%	Mn/Al wt%/wt%	V/Al ppm/wt%	Al_{leach} wt%	$(V/Al)_{leach}$ ppm/wt%	$\varepsilon\ ^{205}Tl_{auth}$ ε -unit	2 SD ε -unit	N	$\delta\ ^{51}V_{auth}$ ‰	2 SD ‰	N
16	0–2	Oxic	5.45	470	2.94	110	125	0.54	0.009	20.18	0.16	79.42	−2.65	0.03	2	−0.79	0.07	2
16	2–4	Oxic	5.45	439	2.72	107	140	0.50	0.008	19.63	0.21	70.69	−2.39	0.43	2	−0.99	0.01	4
16	10–12	Oxic	6.16	469	3.16	119	119	0.51	0.008	19.32	0.22	67.62	−2.67	0.07	2	−0.88	0.10	4
17	2–4	Oxic	7.03	549	4.10	144	156	0.58	0.008	20.48	0.23	67.96	−2.67	0.43	4	−0.87	0.09	3
17	4–6	Oxic	6.95	548	3.98	143	153	0.57	0.008	20.58	0.22	70.23	−2.98	0.39	5	−0.74	0.03	3
17	8–10	Oxic	6.86	571	3.84	140	159	0.56	0.008	20.41	0.21	70.06	−2.78	0.28	2	−1.60	0.07	2
17	12–14	Oxic	6.91	579	4.02	142	173	0.58	0.008	20.55	0.18	73.02	−3.03	0.45	2			
3	2–4	Oxic	8.27	523	3.99	141	162	0.48	0.006	17.05	0.16	66.08	−2.45	0.28	3	−0.86	0.06	2
4	0–2	Oxic	6.08	530	3.04	135	215	0.50	0.009	22.20	0.18	67.61	−2.28	0.20	3	−1.56	0.16	5
4	2–4	Oxic	6.64	520	2.93	133	233	0.44	0.008	20.03			−3.06	0.30	2	−1.27	0.06	4
3	4–6	Suboxic	7.78	489	4.46	128	249	0.57	0.006	16.45	0.13	58.70	−1.86	0.07	3	−0.94	0.04	2
3	6–8	Suboxic	6.71	1690	5.18	109	252	0.77	0.025	16.24						−1.12		1
3	10–12	Suboxic	7.76	1640	5.03	124	184	0.65	0.021	15.98	0.15	55.68	−2.71	0.24	4	−1.15	0.10	2
3	12–14	Suboxic	7.78	1220	4.74	123	153	0.61	0.016	15.81	0.15	74.53	−2.11	0.36	4	−1.11	0.07	2
4	4–6	Suboxic	6.23	590	4.35	124	226	0.70	0.009	19.90	0.18	82.85	−2.78	0.10	3			
4	6–8	Suboxic	6.2	600	4.56	126	157	0.74	0.010	20.32	0.14	79.74	−1.83	0.20	2	−0.44	0.04	4
4	8–10	Suboxic	5.49	650	4.15	128	191	0.76	0.012	23.32	0.15	70.26	−2.50	0.48	2			
16B	2–4	Suboxic	6.55	505	3.37	124	296	0.51	0.008	18.93	0.16	92.45	−2.50	0.35	2	−1.15	0.05	2
16B	4–6	Suboxic	6.15	489	3.07	112	238	0.50	0.008	18.21	0.18	88.10	−3.33	0.25	7			
16B	8–10	Suboxic	6.17	497	3.06	114	159	0.50	0.008	18.48	0.16	72.75	−2.64	0.03	2	−1.39	0.11	6
9	16–18	Euxinic	0.69	288	0.83	41	122	1.20	0.042	59.42	0.08	468.80	−2.20	0.20	2	−0.50	0.11	2
9	24–26	Euxinic	1.04	298	1.05	62	112	1.01	0.029	59.62	0.06	734.33	−2.58	0.51	6	−0.48	0.06	5
15	8–10	Euxinic	6.77	545	3.62	127	186	0.53	0.008	18.76	0.16	83.40	−2.47	0.21	2			
5	8–10	Euxinic	7.73	706	4.27	136	215	0.55	0.009	17.59	0.17	85.28	−2.87	0.45	2	−0.66	0.12	3
BC21	1	Euxinic	1.45		1.11	39	291	0.76		27.23	0.19	126.64	−2.00	0.35	4	−0.62	0.10	3
BC21	2	Euxinic	3.15		2.51	88	402	0.80		27.89	0.30	141.89	−2.20	0.50	2	−0.55	0.02	3
BC21	3	Euxinic					353				0.34	162.67	−2.20	0.10	4	−0.54	0.10	3
BC21	30	Euxinic					119				0.45	40.52	−2.40	0.10	4	−0.61	0.05	3
BC21	49	Euxinic	4.45		2.24	225	584	0.50		50.66	0.39	420.13	−2.80	0.10	3	−0.27	0.11	3
SCo-1												25.06	−2.82	0.10	4	−0.62	0.11	4
BDH																−1.19	0.12	50

Note: Tl concentration and isotope data of core BC21 were from Owens et al (2017). Bulk concentrations of Al, Fe, Mn, and V were from Lyons and Severmann (2006). SCo-1 is the USGS shale reference material. The 2 SD represents the twice standard deviation of each sample during multiple measurements. The redox conditions of the depositional environments for sediments were defined by the iron speciation (Lyons and Severmann, 2006). The V_{leach} and $(V/Al)_{leach}$ represents V to Al ratio in the leachates V isotope measurement.

reported in ε notation relative to the reference standard NIST SRM 997 using the following equation:

$$\varepsilon^{205}Tl = \left[\frac{\left(\frac{^{205}Tl}{^{203}Tl}\right)_{Sample}}{\left(\frac{^{205}Tl}{^{203}Tl}\right)_{NIST\ SRM\ 997}} - 1\right] \times 10,000 \quad (1)$$

The USGS shale reference material SCo-1 was processed and analyzed with our samples to monitor accuracy. The measured authigenic ε^{205}Tl value (–2.8 ± 0.3; 2 SD, N = 4, Table 1) for SCo-1 was similar to previous studies (–2.9 ± 0.1, –3.0 ± 0.2, and –2.8 ± 0.3; Nielsen et al., 2017; Ostrander et al., 2017; Owens et al., 2017; Bowman et al., 2019; Fan et al., 2020). The reported uncertainty of ε^{205}Tl for all our samples is either the 2 SD of SCo-1 (±0.3) or the measured samples, whichever is larger.

Vanadium isotopes were also analyzed on the MC-ICP-MS (Wu et al., 2016; Wu et al., 2019b; Wu et al., 2019a). To discern the isobaric interferences by other molecular species (e.g., $^{36}Ar^{14}N^{+}$, $^{38}Ar^{14}N^{+}$, and $^{36}Ar^{16}O+$), V isotopes were analyzed on the flat-topped shoulder on the lower mass side of the overlapping V and molecular interference peaks at a medium-resolution (ΔM/M) mode of > 4800 (Nielsen et al., 2016; Wu et al., 2016). Ion beams of ^{49}Ti, ^{50}V, ^{52}Cr, ^{53}Cr, and ^{51}V were collected with Faraday cups connected to 10^{11}, 10^{11}, 10^{11}, 10^{11}, and 10^{10} Ω resistor, respectively. The typical voltage for ^{51}V from a V concentration of 600 ppb is ~120 V.

Since minor amounts of Ti and Cr can cause significant interferences with V isotope measurements, we also monitored the ^{49}Ti/^{51}V and ^{53}Cr/^{51}V ratios and kept these ratios below 0.00005 (Wu et al., 2016). To correct the potential interference of ^{50}V by ^{50}Cr and ^{50}Ti, 100 ppb Cr and 100 ppb Ti standard solutions were run separately before each sequence analysis. The instrumental mass bias factors β for Cr and Ti were estimated using the natural abundances of ^{49}Ti, ^{50}Ti, ^{50}Cr, and ^{53}Cr in the standard solutions. These β values were used to calculate ^{50}Ti and ^{50}Cr signals, which were subtracted from the signal of mass 50 to obtain the intensity of ^{50}V.

Samples were measured using a typical sample-standard bracketing method (Nielsen et al., 2011b). Vanadium isotope compositions are reported in a δnotation of per mil relative to the reference standard Alfa Aesar (AA, from Oxford University) using the following equation:

$$\delta^{51}V = \left[\frac{\left(\frac{^{51}V}{^{50}V}\right)_{Sample}}{\left(\frac{^{51}V}{^{50}V}\right)_{AA}} - 1\right] \times 1,000 \quad (2)$$

Each run of a sample was bracketed by four analyses of the AA solutions to monitor the instrument stability. After every two consecutive runs of each sample, a standard solution BDH was also measured to check the performance and stability of the instrument (Nielsen et al., 2011b). Our measured δ^{51}V of the BDH solution was –1.18 ± 0.11‰ (2 SD, N = 588), which was similar to those reported in previous work (–1.19 ± 0.17‰ and –1.23 ± 0.08‰; Nielsen et al., 2011b; Wu et al., 2016). The USGS shale reference materials SCo-1 was processed along with our samples to monitor the long-term precision and accuracy of our extraction methods. The measured δ^{51}V for SCo-1 was –0.62 ± 0.12‰ (2 SD, N = 4, Table 1), which is within error relative to previously published data (–0.65 ± 0.10‰, 2 SD, N = 13; Wu et al., 2020). The errors of δ^{51}V for all our samples are either the 2 SD of SCo-1 or the measured samples, whichever is larger.

4. RESULTS

4.1. Trace metal concentrations in sediments

Trace metal concentrations are displayed in Table 1 (bulk data from Lyons and Severmann, 2006; authigenic Tl concentration (Tl_{auth}) and V/Al in the leached solution for V isotope measurement from this study). Total or bulk Fe concentrations in oxic and suboxic sediments range from 2.72 to 4.10 wt% and from 3.06 to 5.18 wt%, respectively, while they vary substantially from 0.83 to 4.27 wt% in euxinic sediments. Bulk Mn concentrations in oxic, suboxic, and euxinic sediments range from 439 to 579 ppm, 489 to 1690 ppm, and 288 to 706 ppm, respectively. Bulk V concentrations in both oxic (107–144 ppm) and suboxic (109–128 ppm) sediments show a narrow range, with slightly higher V concentrations in oxic sediments. In contrast, euxinic sediments show significantly larger variations in bulk V concentrations from 39 to 127 ppm.

The bulk Fe/Al and Mn/Al ratios are 0.53 ± 0.05 and 0.008 ± 0.001 wt%/wt% (1 SD, N = 10), respectively, in oxic sediments, which are close to the upper continental crust (UCC) values (0.5 wt%/wt% and 0.007 wt%/wt%; McLennan, 2001). However, these ratios are substantially elevated in most sediment samples from the suboxic (0.63 ± 0.11 wt%/wt% for Fe/Al and 0.012 ± 0.006 wt%/wt% for Mn/Al) and euxinic sites (0.81 ± 0.26 wt%/wt% for Fe/Al and 0.017 ± 0.015 wt%/wt% for Mn/Al) (Table 1). Bulk V/Al ratios are moderately higher than UCC (~13.3 ppm/wt%; McLennan, 2001) in oxic and suboxic sediments, with values of 20.0 ± 1.3 ppm/wt% and 18.4 ± 2.4 ppm/wt%, respectively, but are more significantly enriched in most of the euxinic sediments (35.1 ± 19.4 ppm/wt%).

The average authigenic Tl concentrations leached from oxic, suboxic, and euxinic sediments are 164 ± 36 ppb, 211 ± 49 ppb, and 225 ± 112 ppb, respectively. The V/Al ratios in the leachates ($(V/Al)_{leach}$ in Table 1) are significantly higher than those in the bulk sediment. The average $(V/Al)_{leach}$ ratios in oxic, suboxic, and euxinic sediments are 71 ± 5 ppm/wt%, 74 ± 12 ppm/wt%, and 252 ± 252 ppm/wt%, respectively. The percentages of Al extracted from oxic, suboxic, and euxinic sediments during the cold-leaching procedure for V isotope are 3.0 ± 0.5%, 2.4 ± 0.5%, and 7.6 ± 4.2% (Table 1), respectively.

4.2. Authigenic Tl and V isotopic compositions

Authigenic Tl isotopic compositions ($\varepsilon^{205}Tl_{auth}$) in oxic Black Sea sediments range from –3.1 to –2.3, with a mean value of –2.7 ± 0.3 (1 SD, N = 10, Fig. 2A). $\varepsilon^{205}Tl_{auth}$ in suboxic sediments vary between –3.3 to –1.8, with an average value of –2.4 ± 0.5 (1 SD, N = 10). $\varepsilon^{205}Tl_{auth}$ in euxinic sediments vary between –2.9 and –2.0, with a mean value of –2.4 ± 0.3 (1 SD, N = 8). Nearly all of the analyzed

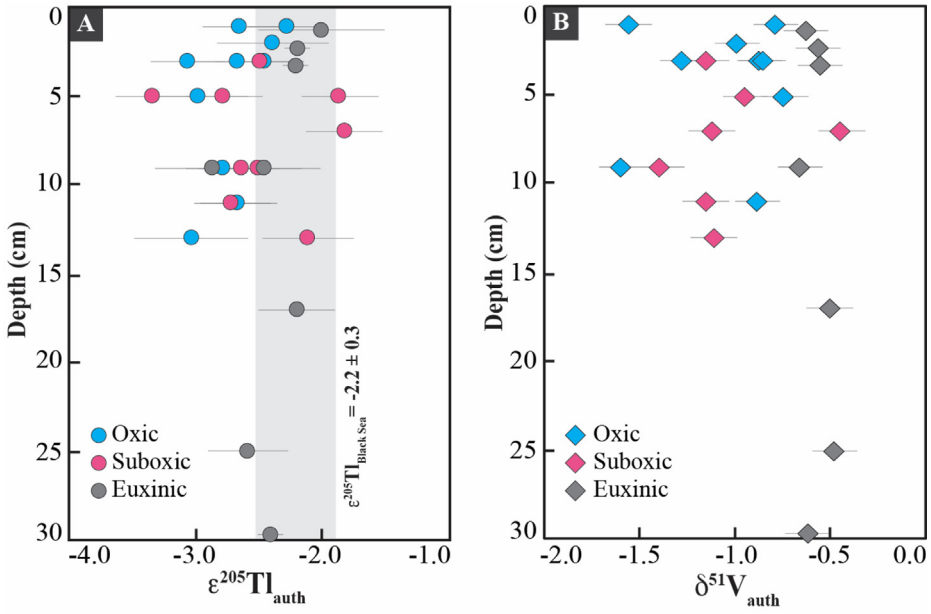

Fig. 2. Sediment depth profiles of authigenic (A) Tl ($\varepsilon^{205}Tl_{auth}$, circles) and (B) V ($\delta^{51}V_{auth}$, diamonds) isotopic compositions in oxic (blue), suboxic (pink), and euxinic (black) sediments of Black Sea. The gray band in (A) represents the measured ε^{205}Tl (–2.2 ± 0.3) in the oxic surface water Black Sea (Owens et al., 2017).

sediments from the Black Sea have $\varepsilon^{205}Tl_{auth}$ values within error of the reported oxic Black Sea seawater ε^{205}Tl value (–2.2 ± 0.3; Owens et al., 2017), except for four samples (three oxic and one suboxic sample) with slightly lighter $\varepsilon^{205}Tl_{auth}$ values (between –2.9 and –3.3; Fig. 2A).

Authigenic V isotope compositions ($\delta^{51}V_{auth}$) in sediments from the oxic shelf of the Black Sea vary significantly between –1.60 and –0.74‰, with an average value of –1.06 ± 0.33‰ (1 SD, N = 9, Fig. 2B). Authigenic δ^{51}V values in the sediments of the chemocline vary within a relatively tighter range between –1.39 and –0.94‰, except for one point with a significantly higher value of –0.44‰. $\delta^{51}V_{auth}$ values in the euxinic sediments of the deep basin are consistently within a very tight range from –0.48 and –0.66‰, with an average of –0.57 ± 0.06‰ (1 SD, N = 7). Similar to $\varepsilon^{205}Tl_{auth}$, $\delta^{51}V_{auth}$ values do not change with core depth (Fig. 2B and Table 1).

5. DISCUSSION

5.1. Acid leaching effect

The hot- and cold-leaching methods have been shown to be reliable in extracting authigenic Tl and V, respectively, from marine sediments (Nielsen et al., 2011a; Wu et al., 2020). Unfortunately, we did not measure Tl/Al in the leachates. Our V/Al ratios and Al contents in the leachates confirm that the cold-leaching method can effectively extract authigenic V with a limited amount of V contributed by lithogenic phases. The average $(V/Al)_{leach}$ ratios in oxic, suboxic, and euxinic sediments are 71 ± 5 ppm/wt%, 74 ± 12 ppm/wt%, and 252 ± 252 ppm/wt%, respectively, which are significantly higher than the ratios for upper continental crust (~13.6 ppm/wt%; McLennan, 2001). The fractions of Al released from lithogenic phases (3.0 ± 0.5%, 2.4 ± 0.5%, and 7.6 ± 2.4% for oxic, suboxic, and anoxic sediments, respectively) using the cold-leaching method for V isotopes are typically lower than 10%, consistent with Wu et al. (2020). Previous work demonstrated that such small fractions of the dissolution of lithogenic phases had negligible effects on the authigenic V isotopic composition (Wu et al., 2020). Thus, we argue that the δ^{51}V values measured using the cold-leaching method represent authigenic V isotopic compositions of the sediments with little contribution from lithogenic components.

5.2. Statistics of $\varepsilon^{205}Tl_{auth}$ and $\delta^{51}V_{auth}$ variations in Black Sea sediments

Our data reveal that $\varepsilon^{205}Tl_{auth}$ values in oxic (–2.7 ± 0.3), suboxic (–2.4 ± 0.5), and euxinic (–2.4 ± 0.3) sediments of Black Sea are statistically indistinguishable (all p-values > 0.05; Table 1 and Fig. 3A), overlapping within error with the oxic surface water of the Black Sea (–2.2 ± 0.3; Owens et al., 2017) and the upper continental crust (–2.1 ± 0.3; Nielsen and Rehkämper, 2011c); Nielsen et al., 2017). In contrast, sedimentary authigenic V isotope compositions in the Black Sea vary with depositional settings. Specifically, $\delta^{51}V_{auth}$ values in oxic and suboxic sediments are statistically the same (–1.06 ± 0.33‰ vs. –1.04 ± 0.30‰; p-value = 0.68, Table 2). However, both sediment types have significantly more negative $\delta^{51}V_{auth}$ values compared to the euxinic sediments (–0.57 ± 0.06‰; both p-values < 0.05, Table 2 and Fig. 3B). Additionally, euxinic sediments have much smaller variations in $\delta^{51}V_{auth}$ compared to the oxic and suboxic sediments in the Black Sea (Fig. 3B).

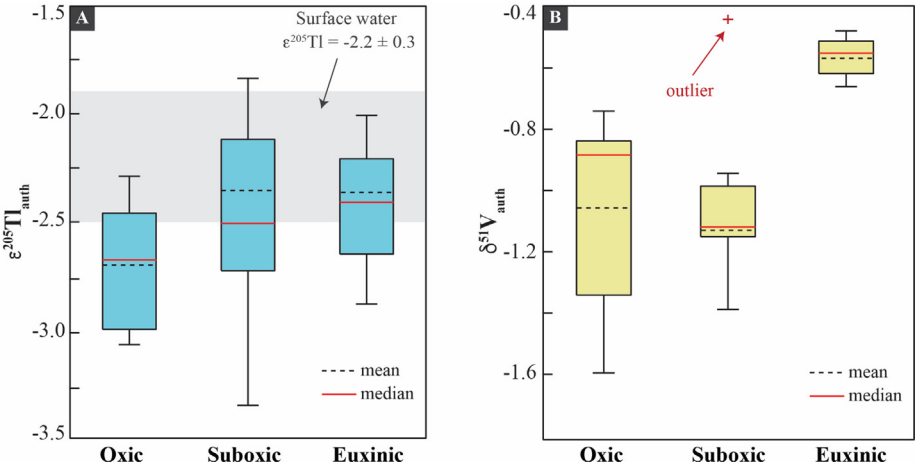

Fig. 3. Box plots of sedimentary authigenic (A) Tl ($\varepsilon^{205}Tl_{auth}$) and (B) V ($\delta^{51}V_{auth}$) isotopic compositions in oxic, suboxic, and euxinic sediments from the Black Sea. Whiskers denote the minimum and maximum of data within 1.5 times the interquartile range from the median. The median and mean values are marked by the solid red and dashed dash lines within the boxes, respectively. The red plus symbol in panel B represents the outlier in the group of $\delta^{51}V_{auth}$ in sediments from the chemocline. The gray band in (A) represents the measured $\varepsilon^{205}Tl$ (–2.2 ± 0.3) in the oxic surface water Black Sea (Owens et al., 2017).

Table 2
Wilcoxon-Mann-Whitney test of authigenic Tl and V isotopic compositions in oxic, suboxic, and euxinic sediments of Black Sea.

	Oxic-Suboxic	Oxic-Euxinic	Suboxic-Euxinic
p-value ($\varepsilon^{205}Tl_{auth}$)	0.16	0.06	0.95
p-value ($\delta^{51}V_{auth}$)	0.68	< 0.01	0.03

5.3. Effects of the redox state of the sedimentary depositional environments

It has been demonstrated that sedimentary authigenic Tl and V isotope compositions in modern marine sediments strongly depend on the redox state of the sedimentary depositional environment given the elements' differences in redox sensitivity (Nielsen et al., 2011a; Nielsen et al., 2013; Nielsen et al., 2017; Owens et al., 2017; Wu et al., 2019b; Wu et al., 2020). Hence, we first discuss the effects of the depositional environment in the Black Sea on variations in Tl and V isotope compositions and then explore the effect of Fe and Mn shuttling on $\varepsilon^{205}Tl_{auth}$ and $\delta^{51}V_{auth}$ values in reducing sediments.

5.3.1. Tl isotopes

Sedimentary $\varepsilon^{205}Tl_{auth}$ values in the Black Sea sediments deposited under oxic, suboxic, and euxinic conditions are statistically indistinguishable and similar to the surface water of this euxinic basin and the upper continental crust. The indistinguishable Tl isotope composition in the most oxic sediments and surface water of the Black Sea appears to contrast with Tl isotope compositions in modern oxic marine sediments (Fe-Mn crust, nodules, and Mn-rich pelagic clays). In the modern ocean, oxic sediments such as Fe-Mn crust and nodules ($\varepsilon^{205}Tl$ = 6–15) and pelagic clays ($\varepsilon^{205}Tl$ = 1–6) have significantly more positive $\varepsilon^{205}Tl$ values relative to homogenous modern seawater (–6.0 ± 0.3), while the predominantly anoxic water-column with sulfide in the upper few centimeters of sediments in the Santa Barbara Basin (–5.5 ± 0.3) and euxinic sediments deposited in the Cariaco Basin (–5.4 ± 0.6) dominantly have $\varepsilon^{205}Tl$ values within error of the modern seawater value (Nielsen et al., 2017; Owens et al., 2017; Fan et al., 2020). The significantly heavy Tl isotope compositions in oxic sediments in the modern ocean results from the burial of Mn oxides, which preferentially accumulate heavy Tl isotopes during surface oxidation of Tl(I) to Tl(III) (Peacock and Moon, 2012; Nielsen et al., 2013; Nielsen et al., 2017).

The lack of preferential accumulation of heavy Tl isotopes in the oxic sediments of the Black Sea most likely results from extensive dissolution of Mn oxides and loss of liberated Tl from the sediments via diffusion because the organic matter contents in these sediments are sufficient to drive Mn reduction but not enough to support appreciable sulfide production and pyrite formation (Force and Cannon, 1988; Lyons et al., 1993). The extensive dissolution of Mn oxides can be inferred by the oxic seawater value in the basin nearly matching the inputs (Owens et al., 2017). The near-crustal Mn/Al (Table 1) in these sediments also suggests limited burial of Mn oxides (Lyons et al., 1993). These oxic sediments from the Black Sea shelf typically contain ~1.3 wt% organic matter and varying amounts of shell materials with a high degree of bioturbation, favorable for reductive dissolution of Mn oxides (Force and Cannon, 1988; Burdige, 1993; Lyons et al., 1993; Lyons and Severmann, 2006; Lenstra et al., 2019; Lenstra et al., 2020). The large benthic flux of Mn (0.31–0.47 mmol m^{-2} d^{-1}) determined in oxic sediments in the northwestern Black Sea suggest the dissolution of Mn oxides and subsequent

diffusion of Mn(II) across the sediment–water interface back into the overlying water column (Friedrich et al., 2002; Lenstra et al., 2020). Since the concentrations of pyrite, the likely host phase of sedimentary authigenic Tl, in our oxic sediments were very low (0.01–0.1 wt%) (Lyons et al., 1993; Lyons and Severmann, 2006), sedimentary Tl associated with Mn oxides would dominantly be released into pore water during the dissolution of Mn oxides and diffuse back into the overlying water column—rather than the isotopic fractionation associated with Mn oxides being captured in pyrite (Lyons et al., 1993). Therefore, we should expect minimal deviations of $\varepsilon^{205}Tl_{auth}$ values as there is limited fractionation from seawater, and values similar to the inputs and crustal material.

Currently, there are no published $\varepsilon^{205}Tl_{auth}$ data that would permit a comprehensive understanding of modern suboxic sediments. The Black Sea suboxic sediments, which contain measurable amounts of pyrite (0.07–3.23 wt%) and in some cases pyrite levels higher than those observed in the euxinic sediments (0.18–1.84 wt%) (Lyons and Berner, 1992; Lyons et al., 1993; Lyons, 1997; Lyons and Severmann, 2006), also record the Tl isotope composition of the surface water of the Black Sea. Since pyrite has been proposed as the predominant host of authigenic Tl in organic-rich sediments (Nielsen et al., 2011a), it is reasonable to expect that the pyrite-rich suboxic sediments from the Black Sea preserve Tl isotope composition of the surface water of this basin (that is, incorporation into pyrite without fractionation) as previously observed in euxinic sediments. Sedimentary $\varepsilon^{205}Tl_{auth}$ values in euxinic sediments of the Black Sea are also indistinguishable from those of the surface water, consistent with data that suggest quantitative removal of Tl from the water column in this basin and the Cariaco Basin (Owens et al., 2017) and as inferred in the anoxic Santa Barbara Basin (Fan et al., 2020). The $\varepsilon^{205}Tl_{auth}$ values do not show correlation with Tl_{auth} for oxic, suboxic, and euxinic sediments (Fig. 4C). In brief, the redox state of the overlying water column has little effect on sedimentary authigenic Tl isotope compositions in the Black Sea, likely due to the rapidly reducing environment in the sediments, which remineralizes Mn oxides in sediments, thus precluding capture of the isotope signal originally associated with Mn oxides. We note that some samples from the suboxic and euxinic sediments show elevated Fe/Al and Mn/Al ratios (Table 1) relative to the upper continental crust (0.5 wt%/wt% and 0.007 wt%/wt%; McLennan, 2001). The potential effect of Fe and Mn shuttle on $\varepsilon^{205}Tl_{auth}$ is discussed below (Section 5.3.1).

5.3.2. V isotopes

In contrast to the Tl isotope data, sedimentary $\delta^{51}V_{auth}$ values in the Black Sea sediments are strongly affected by the redox state of the sedimentary depositional environments, consistent with the most recent study of core-top sediments deposited under various redox conditions (Wu et al., 2020). This previous work revealed that oxic (benthic oxygen > 10 μM), anoxic, and euxinic (Cariaco Basin) sediments have values of –0.9 ± 0.3‰, –0.5 ± 0.2‰, and –0.2 ± 0.2‰, respectively, which are all lower than that of modern seawater (+0.20 ± 0.15‰) (Wu et al., 2019a; Wu et al., 2019b; Wu et al., 2020). Consistent with this finding, our data also documented significantly more positive $\delta^{51}V_{auth}$ values in euxinic sediments (–0.57 ± 0.06‰) compared to oxic and suboxic sediments (–1.06 ± 0.33‰ and –1.04 ± 0.30‰), which are very similar. Additionally, the isotopic offset (0.49 ± 0.34‰) between euxinic and oxic sediments in the Black Sea is also very close to that observed between euxinic sediments from the Cariaco Basin and oxic sediments in the open ocean setting (0.60 ± 0.36‰; Wu et al., 2020). Therefore, we suggest that the redox state of the depositional environments strongly affects sedimentary authigenic V isotopic compositions in the Black Sea sediments, although $\delta^{51}V_{auth}$ values do not correlate with V/Al in the bulk sediments (Fig. 5C).

To further examine relationships between the redox state of the depositional environment and $\delta^{51}V_{auth}$ values in the Black Sea sediments, it would be ideal to analyze the V isotope composition of the surface seawater in this basin. However, the extraordinarily low dissolved V concentrations (<0.75 ppb; Rolison et al., 2017) make the analysis presently impossible given the required sample volume and separation method currently utilized for an isotopic measurement (Wu et al., 2019a). However, the most recent work suggests that the removal of dissolved V from the water column of the restricted Cariaco Basin follows a Rayleigh fractionation model with an intrinsic isotope fractionation of –0.7‰ (Wu et al., 2020). Although the Black Sea is more restricted with a longer deep water renewal time than the Cariaco Basin (400–2,000 years vs. 100 years) and much higher total dissolved H_2S concentration (up to ~400 μM

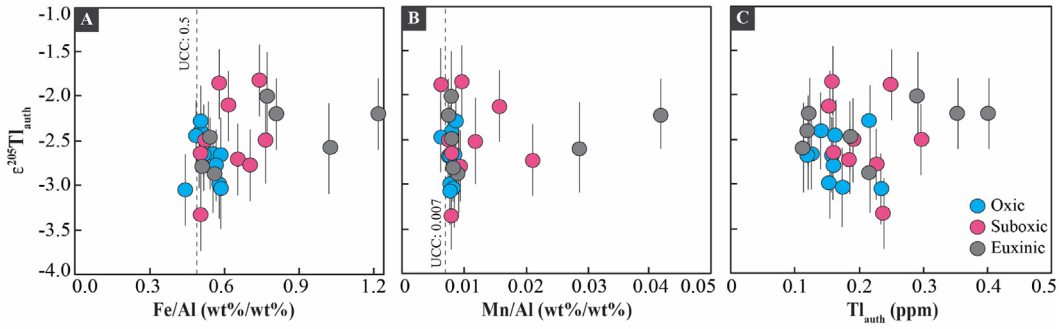

Fig. 4. Cross plots of sedimentary $\varepsilon^{205}Tl_{auth}$ versus bulk Fe/Al (A), Mn/Al (B), and authigenic Tl (Tl_{auth}) (c) in oxic (blue), suboxic (pink), and euxinic (black) sediments of Black Sea. The dashed lines in (A) and (B) represent the Fe/Al, Mn/Al, and V/Al ratios in the upper continental crust (UCC; McLennan, 2001).

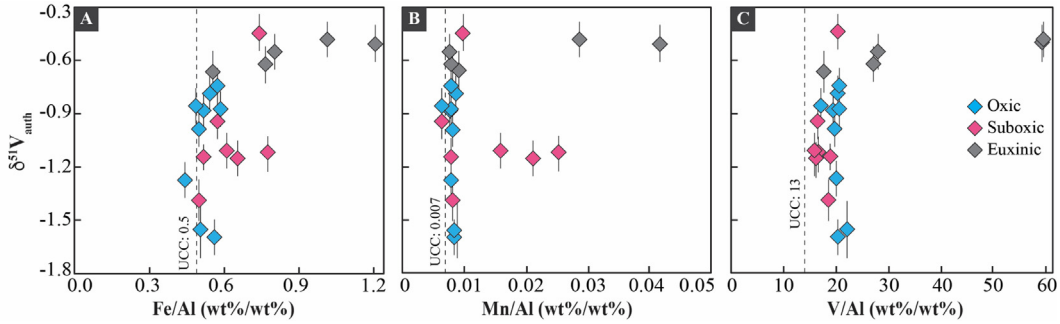

Fig. 5. Cross plots of sedimentary $\delta^{51}V_{auth}$ versus bulk Fe/Al (A), Mn/Al (B), and V/Al (C) in oxic (blue), suboxic (pink), and euxinic (black) sediments of Black Sea. The dashed lines in (A), (B), and (C) represent the Fe/Al, Mn/Al, and V/Al ratios in upper continental crust (UCC; McLennan, 2001).

vs. ~60 μM), depletion of dissolved V in the deep water column relative to the surface seawater is nearly the same (~67% vs. ~65% for the Black Sea and Cariaco Basin, respectively; Emerson and Huested, 1991; Algeo and Lyons, 2006; Rolison et al., 2017).

If we assume that the Black Sea follows the same pattern of V isotope fractionation as the Cariaco Basin with negligible effects on $\delta^{51}V_{auth}$ via Fe and Mn shuttling into euxinic sediments, the inferred Black Sea surface seawater V isotope composition would be about –0.17‰. If correct, the V isotope offsets in the oxic ($\Delta^{51}V_{oxic} = \delta^{51}V_{oxic} - \delta^{51}V_{seawater}$) and suboxic ($\Delta^{51}V_{suboxic} = \delta^{51}Vs_{suboxic} - \delta^{51}V_{seawater}$) sediments relative to the Black Sea surface water would be about –0.89 ± 0.33‰ and –0.87 ± 0.30‰, respectively. The inferred $\Delta^{51}V_{suboxic}$ in the Black Sea is similar to the isotopic offset observed in modern core-top sediments deposited under oxygen-deficient bottom waters (bottom water $[O_2] < 10$ μM and no H_2S) in open marine settings (–0.9 ± 0.2‰; Wu et al., 2020). In contrast, the inferred value for $\Delta^{51}V_{oxic}$ (=–0.89 ± 0.33‰) in the Black Sea appears to be statistically smaller (*p*-value of the non-parametric Student's t-test of these two groups of data is 0.0036) than that determined for the modern oceans (–1.1 ± 0.3‰; Wu et al., 2020). The smaller $\Delta^{51}V_{oxic}$ values in the oxic sediments of the Black Sea relative to modern open oceans (Wu et al., 2020) likely results from differences in the mineralogy of sedimentary Fe and Mn oxides. An increase in V isotope fractionation between Fe-Mn crust and seawater is associated with increasing molar Mn/Fe ratios (Wu et al., 2019b), suggesting that Mn oxides might cause larger V isotope fractionation than Fe oxides. If this is correct, we should expect a small $\Delta^{51}V_{oxic}$ in the Black Sea (with almost no burial of Mn oxides in the oxic sediments) compared to modern open marine settings (e.g., pelagic sediments with the presence of both Fe and Mn oxides; Wu et al., 2020). $\Delta^{51}V_{oxic}$ values in the Black Sea and modern oceans are different because of varying impacts of oxide burial; however, our results suggest that depositional redox most likely controlled sedimentary authigenic V isotope difference for the two redox extremes by some process other than contributions from Fe and Mn shuttling. This assertion is developed further in discussions that follow (Section 5. 3. 2).

The significantly lighter authigenic V isotope compositions in oxic and suboxic sediments (relative to euxinic sediments) in the Black Sea most likely result from an authigenic accumulation of V associated with Fe oxides, which preferentially adsorb isotopically light V isotopes (Wu et al., 2015; Wu et al., 2019b; Wu et al., 2020). Recent work found that Fe and Mn in suspended particles in the bottom waters across the shelf of the Black Sea were composed mainly of ferrihydrite and reducible Fe-oxides (>90% of the total Fe, and MnO_2 (20–60% of the total Mn; Yigiterhan et al., 2011; Lenstra et al., 2019; Lenstra et al., 2020). The strong correlations between V, Fe, and Mn in sinking particles suggest that V scavenged by Fe and Mn oxides are likely the main process for the authigenic accumulation of V in oxic and suboxic sediments across the shelf of the Black Sea (Yigiterhan et al., 2011). Although early diagenesis causes significant reductive dissolution of Fe and Mn oxides in these sediments, reprecipitation of Fe oxides can re-adsorb part of the V released to pore water during reductive dissolution of these oxides (Lyons and Severmann, 2006; Lenstra et al., 2019; Lenstra et al., 2020). Wu et al. (2020) suggested that such processes during early diagenesis did not alter the primary V isotopic signals in oxic sediments. Therefore, we argue that the lighter $\delta^{51}V_{auth}$ values in oxic and suboxic sediments (relative to euxinic sediments) preserve the isotopically light V delivered by particulate Fe and Mn oxides.

5.4. Effects of Fe and/or Mn shuttle

5.4.1. Tl isotopes

The $\varepsilon^{205}Tl_{auth}$ values in the Black Sea sediments are predominantly similar to the surface water of this basin, suggesting little or negligible effects from an Fe and/or Mn shuttle. Given that Fe oxides are not known to cause surface oxidation of Tl(I) to Tl(III), Nielsen et al. (2013) predicted and demonstrated little or no Tl isotope fractionation during Tl adsorption to Fe oxides. Instead, the chemical process that drives Tl isotope fractionation is adsorption to Mn oxides. Thus, as expected, Fe shuttling did not affect the Tl isotope compositions in sediments even though there is a strong and active lateral and vertical transport of Fe in the Black Sea (as manifested in elevated Fe/Al ratios, Fig. 4A) (Wijsman et al., 2001; Raiswell and Anderson, 2005; Lyons and Severmann, 2006; Severmann et al., 2008; Eckert et al., 2013; Lenstra et al., 2019).

The Mn/Al ratios in almost all of our Black Sea sediments are close to the upper continental crust (0.007 wt %/wt%; McLennan, 2001) except for a few samples from the suboxic (three) and euxinic (two) sediments (0.12–0.42) with significant enrichments in Mn (Fig. 4B and Table 1). Consistent with our expectation, samples with near-crustal Mn/Al ratios have $\varepsilon^{205}Tl_{auth}$ values close to the surface water of the Black Sea and the upper continental crust (Nielsen and Rehkämper, 2011c; Nielsen et al., 2017; Owens et al., 2017). Unexpectedly, however, $\varepsilon^{205}Tl_{auth}$ values in those samples with significant Mn enrichments (Force and Cannon, 1988; Lyons and Severmann, 2006) are also near the surface water of the Black Sea, suggesting little effect of a Mn shuttle on the sedimentary $\varepsilon^{205}Tl_{auth}$, likely because of reductive loss of Mn oxides in the water column or sediments and the lack of a Tl retention pathway in the suboxic sediments of the oxic shelf.

5.4.2. V isotopes

The significant enrichments of Fe, Mn, and V in most euxinic sediments (Fig. 5) in the Black Sea seem to suggest that Fe and Mn shuttling might affect $\delta^{51}V_{auth}$ values. Since Fe-Mn crusts and nodules preferentially accumulate lighter V isotopes in modern oceans with an isotope fractionation of 1.2 ± 0.2‰ (Wu et al., 2019b), we would expect authigenic V isotope compositions in euxinic sediments to decrease with an increase in the Fe/Al and/or Mn/Al ratios. However, all the $\delta^{51}V_{auth}$ values in the euxinic sediments of the Black Sea fall within a narrow range of values of –0.57 ± 0.06‰ (1 SD, N = 7), independent of the significant variations in Fe/Al and/or Mn/Al ratios (Table 1 and Fig. 5). These observations suggest that Fe and Mn shuttling have minor or little effect on $\delta^{51}V_{auth}$ values in euxinic sediments in the Black Sea. In short, $\delta^{51}V_{auth}$ in the Black Sea sediments most likely reflect the local redox state of the sedimentary depositional environments with little impact by Fe and Mn shuttling.

5.5. Implications for the effect of Fe and Mn shuttle on sedimentary Tl and V isotopic signature

Although Fe/Al and Mn/Al ratios and Fe isotopes have demonstrated strong effects from the 'benthic Fe and Mn redox shuttle' in the Black Sea (Fig. 6A; Wijsman et al., 2001; Anderson and Raiswell, 2004; Raiswell and Anderson, 2005; Lyons and Severmann, 2006; Severmann et al., 2008; Dellwig et al., 2010; Eckert et al., 2013; Lenstra et al., 2019; Lenstra et al., 2020), our data reveal that such processes do not affect sedimentary authigenic Tl and V isotopic compositions. The lack of Fe and Mn shuttle effects on Tl and V isotopes in the strongly restricted Black Sea most likely results from the shallow chemocline (~100 m water depth in the center of the bain) within a stable redox-stratified water column of 2200 m in depth (e.g., Algeo and Lyons, 2006) and the specific geochemical processes that scavenge Tl and V into euxinic sediments in the Black Sea.

Because of the long renewal time (400–2000 years) of deep water in the Black Sea with high total dissolved hydrogen sulfide concentrations (up to 600 μM), particulate Fe and Mn oxides formed within the chemocline and/or mobilized from the shelf are completely dissolved below the chemocline before reaching the sediment/water interface (Spencer and Brewer, 1971; Brewer and Spencer, 1974; Lewis and Landing, 1991; Algeo and Tribovillard, 2009; Pakhomova et al., 2009; Dellwig et al., 2010; Yigiterhan et al., 2011; Lenstra et al., 2019; Lenstra et al., 2020), releasing particulate V and Tl associated with these oxides back into the reducing water column before they reach the sediment–water interface (Fig. 6A). The shallow chemocline in the Black Sea, thus, precludes the effect of Fe and Mn shuttles on Tl and V isotope signatures in the euxinic sediments of this basin via the 'particulate shuttle' pathway (Little et al., 2015).

More importantly, the geochemical processes scavenging dissolved Tl and V from euxinic water columns into sediments determine whether the 'benthic Fe and Mn redox shuttle' can affect Tl and V isotope signatures in euxinic sediments. The near-quantitative removal of dissolved Tl below the chemocline of the Black Sea (Owens et al., 2017) precludes the transport of Tl into the deep euxinic basins via the benthic Fe and Mn redox shuttle, resulting in minor effects on $\varepsilon^{205}Tl_{auth}$ in euxinic sediments. In contrast, about 67% of dissolved V in the Black Sea was removed into sediments (Rolison et al., 2017). The removal of dissolved V is likely associated with the reduction of vanadate to vanadyl in the reducing water column of the Black Sea and subsequent incorporation of vanadyl into particulate organic matter through either an abiotic or biotic pathway (Ohnemus et al., 2017; Nielsen, 2020). This process likely imparts V isotope fractionation like that observed in the euxinic sediments of the Cariaco Basin, where lighter V isotopes were preferentially removed by reducing sediments (Wu et al., 2020). The partial removal of dissolved V in the sulfidic water column into sediments in the Black Sea would dampen the effect of the benthic Fe and Mn redox shuttle on V isotopic compositions in euxinic sediments (Fig. 6A). The incomplete removal of dissolved V in the Black Sea is likely associated with vanadyl uptake by particulate organic matter and kinetically unfavorable reduction of vanadyl to insoluble trivalent V species (Nielsen, 2020; Wanty and Goldhaber, 1992). Unlike dissolved V, Fe, Mn, and Mo precipitate as low-solubility minerals such as greigite (Fe_3S_4), pyrite (FeS_2), rhodochrosite ($MnCO_3$), and $FeMoS_4$ (Fig. 6A; Lewis and Landing, 1991; Lyons, 1997; Anderson and Raiswell, 2004; Lyons and Severmann, 2006; Helz et al., 2011; Little et al., 2015; Vorlicek et al., 2018), leading to near-quantitative removal of dissolved Fe and Mn from the euxinic water columns and capture of the effect of the benthic Fe and Mn redox shuttle by euxinic sediments. Consequently, the benthic Fe and Mn redox shuttle can significantly affect authigenic enrichments of Fe, Mn, and Fe isotopic compositions in euxinic sediments in the Black Sea but has little effect on the authigenic enrichments in Tl and V and their isotopic compositions in euxinic sediments.

Although our results document no significant impact from Fe and Mn shuttling to sediments in the strongly restricted Black Sea, they do not exclude the potential

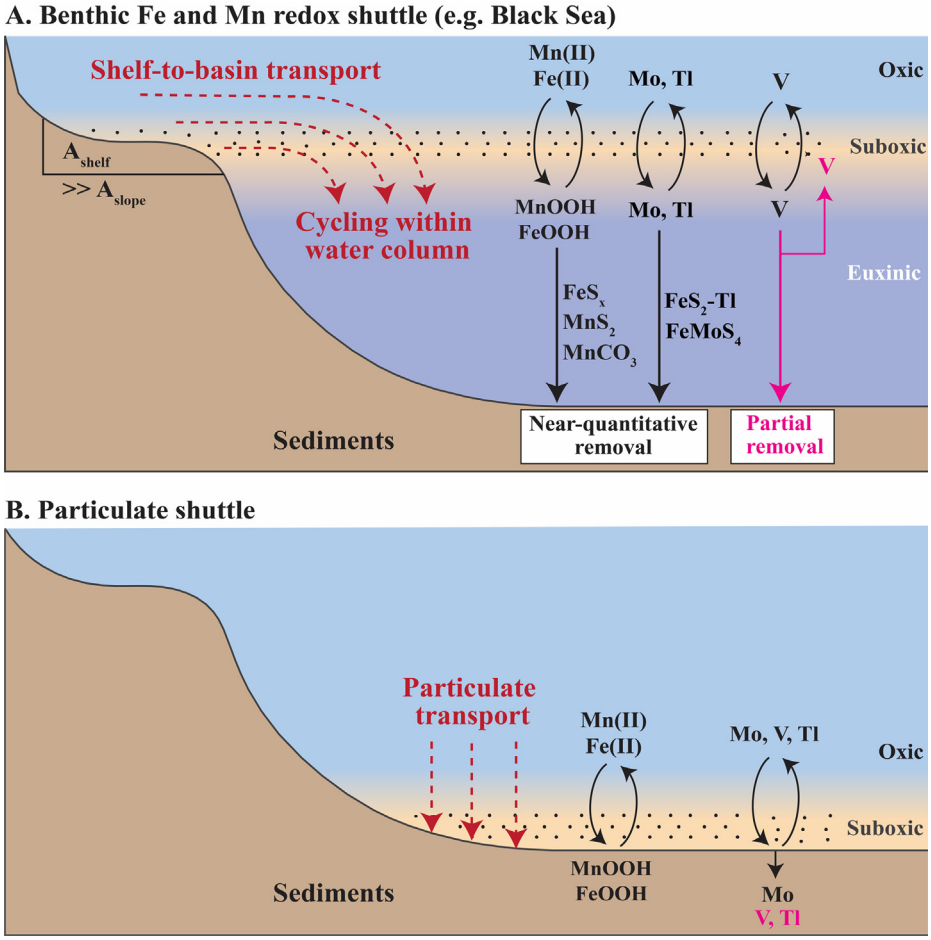

Fig. 6. Concept models of the 'benthic Fe and Mn redox shuttle' (A) and the 'particulate shuttle' (B) and their effects on Mo, Tl, and V cycling. FeS_x represent different types of Fe-S minerals such as pyrite, FeS, and greigite (Fe_3S_4). $FeMoS_4$ is a Mo precipitate formed in the euxinic water column (Helz et al., 2011; Vorlicek et al., 2018). FeS_2-Tl means that Tl is likely scavenged from the sulfidic water column by pyrite (Nielsen et al., 2011). The pink colored fonts of V and Tl in panel B indicate that the effect of the 'particulate shuttle' on sedimentary V and Tl isotope signatures remains unknown.

effect of other types of Fe and Mn shuttles, such as the 'particulate shuttle' (Fig. 6B), on sedimentary authigenic Tl and V enrichments and their isotopic compositions in other marine settings, such as modern marginal OMZs, reducing coastal basins, etc. For example, weakly restricted basins (e.g., Baltic Sea) with a regular inflow of oxygenated seawater and oxygen minimum zones at open-marine continental margins (e.g., Peru upwelling area) have been proposed as ideal locations for the operation of Fe and Mn shuttles and modern marine analogs for ancient redox-stratified oceans (Reinhard et al., 2009; Kendall et al., 2010; Li et al., 2010; Poulton et al., 2010; Scholz et al., 2011, 2013, 2017; Ostrander et al., 2019b). These marine settings have documented significant enrichments in authigenic Fe, Mn, and Mo accompanied by lighter $\delta^{98}Mo_{auth}$ values in organic-rich sediments (relative to the surface waters) and large fluxes of particulate Fe and Mn oxides with associated Mo in bottom waters via the 'particulate shuttle', pointing to the operation of Fe and Mn shuttling that substantially enhances Mo burial (e.g., Fehr et al., 2010; Scholz et al., 2011, 2013, 2017, 2018; Jilbert and Slomp, 2013; Eroglu et al., 2020). The strong correlations of V with Fe and Mn oxides in sinking particles in the Black Sea and Baltic sea (e.g., Yigiterhan et al., 2011; Bauer et al., 2017) and strong affinity of Tl to hydrogenous Mn oxides (Rehkämper et al., 2002; Nielsen et al., 2013) suggests the potential effects of Fe and Mn shuttling on sedimentary authigenic Tl and V isotopic signals should be further explored. Our conclusions, however, point to the likelihood of limited impacts in highly and persistently reducing settings analogous to the Black Sea.

6. CONCLUSIONS

Our data reveal statistically identical $\varepsilon^{205}Tl_{auth}$ values in oxic, suboxic, and euxinic sediments in the Black Sea but variable sedimentary $\delta^{51}V_{auth}$ values, with heavier V isotope compositions in euxinic sediments. Sedimentary $\varepsilon^{205}Tl_{auth}$ is not affected by either the redox state of the overlying water or Fe and Mn shuttling likely due to the highly reducing conditions of the deep basin and the suboxic pore water systems of the oxic shelf. The absence of heavier Tl isotope

compositions in oxic sediments relative to the surface seawater of the Black Sea results from environmental conditions that are unfavorable for delivery or long-term burial of Mn oxides. In contrast, sedimentary $\delta^{51}V_{auth}$ is predominantly controlled by the redox state of the depositional environment but with little effect from Fe and Mn shuttling. The lack of Fe and Mn shuttling effects on sedimentary authigenic Tl and V isotopic signals in the Black Sea most likely results from the shallow chemocline in the strongly restricted euxinic basin and thus the lack of Fe and Mn particulate oxide delivery to the sediments. Our work, however, motivates further investigation of Fe and Mn shuttling effects on sedimentary $\varepsilon^{205}Tl_{auth}$ and $\delta^{51}V_{auth}$ in weakly restricted basins and oxygen minimum zones on continental margins that favor Fe and Mn shuttling. Such settings may be more representative of many or most redox-stratified oceans in deep time, which may have been less reducing (that is, less persistently and highly sulfidic) than the modern Black Sea.

Declaration of Competing Interest

The authors declare that they have no known competing financial interests or personal relationships that could have appeared to influence the work reported in this paper.

ACKNOWLEDGEMENTS

G. White is thanked for instrumentation troubleshooting at the MagLab. The work was funded by grants from NASA Exobiology 80NSSC18K1532 awarded to JDO and JDO thanks the Alfred P. Sloan Foundation. The NASA Astrobiology Institute under Cooperative Agreement No. NNA15BB03A issued through the Science Mission Directorate Contributions and the NASA Interdisciplinary Consortia for Astrobiology Research provided support to Lyons. JDO is supported by the National High Magnetic Field Laboratory (Tallahassee, Florida), which is funded by the National Science Foundation Cooperative Agreement No. DMR1644779 and the State of Florida. We appreciated the insightful comments and suggestions from three anonymous reviewers', which have significantly improved this manuscript.

APPENDIX A. SUPPLEMENTARY DATA

Supplementary data to this article can be found online at https://doi.org/10.1016/j.gca.2021.11.010.

REFERENCES

Algeo T. J. and Lyons T. W. (2006) Mo-total organic carbon covariation in modern anoxic marine environments: Implications for analysis of paleoredox and paleohydrographic conditions. *Paleoceanography* **21**.

Algeo T. J. and Tribovillard N. (2009) Environmental analysis of paleoceanographic systems based on molybdenum-uranium covariation. *Chem. Geol.* **268**, 211–225.

Algeo T. J. and Li C. (2020) Redox classification and calibration of redox thresholds in sedimentary systems. *Geochim. Cosmochim. Acta* **287**, 8–26.

Anbar A. D. (2004) Molybdenum stable isotopes: Observations, interpretations and directions. *Rev. Mineral. Geochemistry* **55**, 429–454.

Anderson T. F. and Raiswell R. (2004) Sources and mechanisms for the enrichment of highly reactive iron in euxinic Black Sea sediments. *Am. J. Sci.* **304**, 203–233.

Arthur M. A., Dean W. E., Neff E. D., Hay B. J., King J. and Jones G. (1994) Varve calibrated records of carbonate and organic carbon accumulation over the last 2000 years in the Black Sea. *Global Biogeochem. Cycles* **8**, 195–217.

Barling J. and Anbar A. D. (2004) Molybdenum isotope fractionation during adsorption by manganese oxides. *Earth Planet. Sci. Lett.* **217**, 315–329.

Barling J., Arnold G. L. and Anbar A. D. (2001) Natural mass-dependent variations in the isotopic composition of molybdenum. *Earth Planet. Sci. Lett.* **193**, 447–457.

Bauer S., Blomqvist S. and Ingri J. (2017) Distribution of dissolved and suspended particulate molybdenum, vanadium, and tungsten in the Baltic Sea. *Mar. Chem.* **196**, 135–147.

Bowman C. N., Young S. A., Kaljo D., Eriksson M. E., Them T. R., Hints O., Martma T. and Owens J. D. (2019) Linking the progressive expansion of reducing conditions to a stepwise mass extinction event in the late Silurian oceans. *Geology* **47**, 968–972.

Brewer P. G. and Spencer D. W. (1974) Distribution of some trace elements in the Black Sea and their flux between dissolved and particulate phases. In *The Black Sea-Geology, Chemistry and Biology* (eds. E. T. Degens and D. A. Ross). American Association of Petroleum Geologists, Tusla, OK, pp. 137–143.

Brüske A., Weyer S., Zhao M. Y., Planavsky N. J., Wegwerth A., Neubert N., Dellwig O., Lau K. V. and Lyons T. W. (2020) Correlated molybdenum and uranium isotope signatures in modern anoxic sediments: Implications for their use as paleoredox proxy. *Geochim. Cosmochim. Acta* **270**, 449–474.

Bura-Nakić E., Andersen M. B., Archer C., de Souza G. F., Marguš M. and Vance D. (2018) Coupled Mo-U abundances and isotopes in a small marine euxinic basin: Constraints on processes in euxinic basins. *Geochim. Cosmochim. Acta* **222**, 212–229.

Burdige D. J. (1993) The biogeochemistry of manganese and iron reduction in marine sediments. *Earth Sci. Rev.* **35**, 249–284.

Cole D. B., Mills D. B., Erwin D. H., Sperling E. A., Porter S. M., Reinhard C. T. and Planavsky N. J. (2020) On the co-evolution of surface oxygen levels and animasl. *Geobiology* **18**, 260–281.

Dellwig O., Leipe T., März C., Glockzin M., Pollehne F., Schnetger B., Yakushev E. V., Böttcher M. E. and Brumsack H. J. (2010) A new particulate Mn-Fe-P shuttle at the redoxcline of anoxic basins. *Geochim. Cosmochim. Acta* **74**, 7100–7115.

Eckert S., Brumsack H. J., Severmann S., Schnetger B., März C. and Fröllje H. (2013) Establishment of euxinic conditions in the Holocene Black Sea. *Geology* **41**, 431–434.

Emerson S. R. and Huested S. S. (1991) Ocean anoxia and the concentrations of molybdenum and vanadium in seawater. *Mar. Chem.* **34**, 177–196.

Eroglu S., Scholz F., Frank M. and Siebert C. (2020) Influence of particulate versus diffusive molybdenum supply mechanisms on the molybdenum isotope composition of continental margin sediments. *Geochim. Cosmochim. Acta* **273**, 51–69.

Fan H., Nielsen S. G., Owens J. D., Auro M., Shu Y., Hardisty D. S., Horner T. J., Bowman C. N., Young S. A. and Wen H. (2020) Constraining oceanic oxygenation during the Shuram excursion in South China using thallium isotopes. *Geobiology*, 1–17.

Fehr M. A., Andersson P. S., Hålenius U., Gustafsson O. and Morth C. M. (2010) Iron enrichments and Fe isotopic compositions of surface sediments from the Gotland Deep, Baltic Sea. *Chem. Geol.* **277**, 310–322.

Force E. R. and Cannon W. F. (1988) Depositional model for shallow-marine manganese deposits around black shale basins. *Econ. Geol.* **83**, 93–117.

Friedrich J., Dinkel C., Friedl G., Pimenov N., Wijsman J., Gomoiu M. T., Cociasu A., Popa L. and Wehrli B. (2002) Benthic nutrient cycling and diagenetic pathways in the northwestern Black Sea. *Estuar. Coast. Shelf Sci.* **54**, 369–383.

Goldberg T., Archer C., Vance D. and Poulton S. W. (2009) Mo isotope fractionation during adsorption to Fe (oxyhydr)oxides. *Geochim. Cosmochim. Acta* **73**, 6502–6516.

Hein J. R. and Koschinsky A. (2013) *Deep-Ocean Ferromanganese Crusts and Nodules*. 2nd ed., Published by Elsevier Inc.

Helz G. R., Bura-Nakić E., Mikac N. and Ciglenečki I. (2011) New model for molybdenum behavior in euxinic waters. *Chem. Geol.* **284**, 323–332.

Herrmann A. D., Kendall B., Algeo T. J., Gordon G. W., Wasylenki L. E. and Anbar A. D. (2012) Anomalous molybdenum isotope trends in Upper Pennsylvanian euxinic facies: Significance for use of δ 98 Mo as a global marine redox proxy. *Chem. Geol.* **324–325**, 87–98.

Jenkins W, Tracer of Ocean Mixing, In: Elderfield H, The Oceans and Marine Geochemistry, 2003, Pergamon, 223–246.

Jilbert T. and Slomp C. P. (2013) Iron and manganese shuttles control the formation of authigenic phosphorus minerals in the euxinic basins of the Baltic Sea. *Geochim. Cosmochim. Acta* **107**, 155–169.

Kendall B., Dahl T. W. and Anbar A. D. (2017) The stable isotope geochemistry of molybdenum. *Rev. Mineral. Geochem.* **82**, 683–732.

Kendall B., Reinhard C. T., Lyons T. W., Kaufman A. J., Poulton S. W. and Anbar A. D. (2010) Pervasive oxygenation along late Archaean ocean margins. *Nat. Geosci.* **3**, 647–652.

Knoll A. H. and Sperling E. A. (2014) Oxygen and animals in Earth history. *Proc. Natl. Acad. Sci. U. S. A.* **111**, 3907–3908.

Kurzweil F., Wille M., Gantert N., Beukes N. J. and Schoenberg R. (2016) Manganese oxide shuttling in pre-GOE oceans – evidence from molybdenum and iron isotopes. *Earth Planet. Sci. Lett.* **452**, 69–78.

Lenstra W. K., Hermans M., Séguret M. J. M., Witbaard R., Behrends T., Dijkstra N., van Helmond N. A. G. M., Kraal P., Laan P., Rijkenberg M. J. A., Severmann S., Teacă A. and Slomp C. P. (2019) The shelf-to-basin iron shuttle in the Black Sea revisited. *Chem. Geol.* **511**, 314–341.

Lenstra W. K., Séguret M. J. M., Behrends T., Groeneveld R. K., Hermans M., Witbaard R. and Slomp C. P. (2020) Controls on the shuttling of manganese over the northwestern Black Sea shelf and its fate in the euxinic deep basin. *Geochim. Cosmochim. Acta* **273**, 177–204.

Lewis B. L. and Landing W. M. (1991) The biogeochemistry of manganese and iron in the Black Sea. *Deep Sea Res* Available at:. *Part A. Oceanogr. Res. Pap.* **38**, S773–S803 http://linkinghub.elsevier.com/retrieve/pii/S0198014910800093.

Li C., Love G. D., Lyons T. W., Fike D. A., Sessions A. L. and Chu X. (2010) A stratified redox model for the ediacaran ocean. *Science* **328**, 80–83.

Little S. H., Vance D., Lyons T. W. and McManus J. (2015) Controls on trace metal authigenic enrichment in reducing sediments: Insights from modern oxygen-deficient settings. *Am. J. Sci.* **315**, 77–119.

Lyons T. W. (1997) Sulfur isotopic trends and pathways of iron sulfide formation in upper holocene sediments of the anoxic black sea Available at:. *Geochim. Cosmochim. Acta* **61**, 3367–3382 http://linkinghub.elsevier.com/retrieve/pii/S0016703797001749.

Lyons T. W. (1991) Upper Holocene sediments of the Black Sea: summary of Leg 4 box cores (1988 Black Sea Oceanographic Expedition), in *Black Sea Oceanography* (eds. E. Izdar and J. W. Murray) Kluwer Academic, Norwell. Mass. pp. 401-441.

Lyons T. W. and Berner R. A. (1992) Carbon-sulfur-iron systematics of the uppermost deep-water sediments of the Black Sea. *Chem. Geol.* **99**, 1–27.

Lyons T. W., Berner R. A. and Anderson R. F. (1993) Evidence for large pre-industrial perturbations of the Black Sea chemocline. *Nature* **365**, 538–540.

Lyons T. W. and Severmann S. (2006) A critical look at iron paleoredox proxies: New insights from modern euxinic marine basins. *Geochim. Cosmochim. Acta* **70**, 5698–5722.

McLennan S. M. (2001) Relationships between the trace element composition of sedimentary rocks and upper continental crust. *Geochemistry, Geophys. Geosystems*. **2**.

McManus J., Berelson W. M., Severmann S., Poulson R. L., Hammond D. E., Klinkhammer G. P. and Holm C. (2006) Molybdenum and uranium geochemistry in continental margin sediments: Paleoproxy potential. *Geochim. Cosmochim. Acta* **70**, 4643–4662.

McManus J., Nägler T. F., Siebert C., Wheat C. G. and Hammond D. E. (2002) Oceanic molybdenum isotope fractionation: Diagenesis and hydrothermal ridge-flank alteration. *Geochemistry, Geophys. Geosystems* **3**, 1–9.

Millero F. J. (2013) *Chemical Oceanography*. CRC Press, Boca Raton.

Mills D. B. and Canfield D. E. (2014) Oxygen and animal evolution: Did a rise of atmospheric oxygen "trigger" the origin of animals? *BioEssays* **36**, 1145–1155.

Murray J. (1989) The 1988 Black Sea Oceanographic Expedition: Overview and New Discoveries. *Oceanography* **2**, 15–21.

Nägler T. F., Neubert N., Böttcher M. E., Dellwig O. and Schnetger B. (2011) Molybdenum isotope fractionation in pelagic euxinia: Evidence from the modern Black and Baltic Seas. *Chem. Geol.* **289**, 1–11.

Neubert N., Nägler T. F. and Böttcher M. E. (2008) Sulfidity controls molybdenum isotope fractionation into euxinic sediments: Evidence from the modern Black Sea. *Geology* **36**, 775–778.

Nielsen S. G., Goff M., Hesselbo S. P., Jenkyns H. C., LaRowe D. E. and Lee C. T. A. (2011a) Thallium isotopes in early diagenetic pyrite - A paleoredox proxy? *Geochim. Cosmochim. Acta* **75**, 6690–6704.

Nielsen S. G., Mar-Gerrison S., Gannoun A., LaRowe D., Klemm V., Halliday A. N., Burton K. W. and Hein J. R. (2009a) Thallium isotope evidence for a permanent increase in marine organic carbon export in the early Eocene. *Earth Planet. Sci. Lett.* **278**, 297–307.

Nielsen S. G. (2020) *Vanadium Isotopes: A Proxy for Ocean Oxygen Variations*. Cambridge University Press, Cambridge.

Nielsen S. G., Owens J. D. and Horner T. J. (2016) Analysis of high-precision vanadium isotope ratios by medium resolution MC-ICP-MS. *J. Anal. At. Spectrom.* **31**, 531–536.

Nielsen S. G., Prytulak J. and Halliday A. N. (2011b) Determination of precise and accurate $^{51}V/^{50}V$ isotope ratios by MC-ICP-MS, Part 1: Chemical separation of vanadium and mass spectrometric protocols. *Geostand. Geoanalytical Res.* **35**, 293–306.

Nielsen S. G., and Rehkämper M. (2011c) Thallium isotopes and their application to problems in earth and environmental science. In *Handbook of Environmental Isotope Geochemistry* (ed. M. Baskaran). Springer, pp. 247–270.

Nielsen S. G., Rehkämper M., Porcelli D., Andersson P., Halliday A. N., Swarzenski P. W., Latkoczy C. and Günther D. (2005) Thallium isotope composition of the upper continental crust and rivers–An investigation of the continental sources of dissolved marine thallium. *Geochim. Cosmochim. Acta* **69**, 2007–2019.

Nielsen S. G., Rehkämper M. and Prytulak J. (2017) Investigation and application of thallium isotope fractionation. *Rev. Mineral. Geochemistry* **82**, 759–798.

Nielsen S. G., Wasylenki L. E., Rehkämper M., Peacock C. L., Xue Z. and Moon E. M. (2013) Towards an understanding of thallium isotope fractionation during adsorption to manganese oxides. *Geochim. Cosmochim. Acta* **117**, 252–265.

Nielsen S. G., Williams H. M., Griffin W. L., O'Reilly S. Y., Pearson N. and Viljoen F. (2009b) Thallium isotopes as a potential tracer for the origin of cratonic eclogites. *Geochim. Cosmochim. Acta* **73**, 7387–7398.

Noordmann J., Weyer S., Montoya-Pino C., Dellwig O., Neubert N., Eckert S., Paetzel M. and Böttcher M. E. (2015) Uranium and molybdenum isotope systematics in modern euxinic basins: Case studies from the central Baltic Sea and the Kyllaren fjord (Norway). *Chem. Geol.* **396**, 182–195.

Ohnemus D. C., Rauschenberg S., Cutter G. A., Fitzsimmons J. N., Sherrell R. M. and Twining B. S. (2017) Elevated trace metal content of prokaryotic communities associated with marine oxygen deficient zones. *Limnol. Oceanogr.* **62**, 3–25.

Ostrander C. M., Nielsen S. G., Owens J. D., Kendall B., Gordon G. W., Romaniello S. J. and Anbar A. D. (2019a) Fully oxygenated water columns over continental shelves before the Great Oxidation Event Available at:. *Nat. Geosci.* **12**, 186–192 http://www.nature.com/articles/s41561-019-0309-7.

Ostrander C. M., Owens J. D. and Nielsen S. G. (2017) Constraining the rate of oceanic deoxygenation leading up to a Cretaceous Oceanic Anoxic Event (OAE-2: ~94 Ma) Available at:. *Sci. Adv.*, 1–6 http://advances.sciencemag.org/content/3/8/e1701020.full.

Ostrander C. M., Sahoo S. K., Kendall B., Jiang G., Planavsky N. J., Lyons T. W., Nielsen S. G., Owens J. D., Gordon G. W., Romaniello S. J. and Anbar A. D. (2019b) Multiple negative molybdenum isotope excursions in the Doushantuo Formation (South China) fingerprint complex redox-related processes in the Ediacaran Nanhua Basin Available at:. *Geochim. Cosmochim. Acta* **261**, 191–209 https://linkinghub.elsevier.com/retrieve/pii/S0016703719304260.

Owens J. D., Nielsen S. G., Horner T. J., Ostrander C. M. and Peterson L. C. (2017) Thallium-isotopic compositions of euxinic sediments as a proxy for global manganese-oxide burial. *Geochim. Cosmochim. Acta* **213**, 291–307.

Owens J. D. (2019) *Application of Thallium Isotopes: Tracking Marine Oxygenation Through Manganese Oxide Burial*. Cambridge University Press, Cambridge.

Pakhomova S. V., Rozanov A. G. and Yakushev E. V. (2009) Dissolved and particulate forms of iron and manganese in the redox zone of the Black Sea Available at:. *Oceanology* **49**, 773–787 http://link.springer.com/10.1134/S0001437009060046.

Peacock C. L. and Moon E. M. (2012) Oxidative scavenging of thallium by birnessite: Explanation for thallium enrichment and stable isotope fractionation in marine ferromanganese precipitates. *Geochim. Cosmochim. Acta* **84**, 297–313.

Poulson R. L., Siebert C., McManus J. and Berelson W. M. (2006) Authigenic molybdenum isotope signatures in marine sediments. *Geology* **34**, 617–620.

Poulton S. W., Fralick P. W. and Canfield D. E. (2010) Spatial variability in oceanic redox structure 1.8 billion years ago. *Nat. Geosci.* **3**, 486–490.

Raiswell R. and Anderson T. F. (2005) Reactive iron enrichment in sediments deposited beneath euxinic bottom waters: Constraints on supply by shelf recycling. *Geol. Soc. Spec. Publ.* **248**, 179–194.

Raman A. V., Frieder C. A., Levin L. A., Knoll A. H., Girguis P. R. and Sperling E. A. (2013) Oxygen, ecology, and the Cambrian radiation of animals. *Proc. Natl. Acad. Sci.* **110**, 13446–13451.

Rehkämper M., Frank M., Hein J. R., Porcelli D., Halliday A., Ingri J. and Liebetrau V. (2002) Thallium isotope variations in seawater and hydrogenetic, diagenetic, and hydrothermal ferromanganese deposits. *Earth Planet. Sci. Lett.* **197**, 65–81.

Rehkämper M. and Halliday A. N. (1999) The precise measurement of Tl isotopic compositions by MC-ICPMS: Application to the analysis of geological materials and meteorites. *Geochim. Cosmochim. Acta* **63**, 935–944.

Rehkämper M. and Nielsen S. G. (2004) The mass balance of dissolved thallium in the oceans. *Mar. Chem.* **85**, 125–139.

Reinhard C. T., Planavsky N. J., Olson S. L., Lyons T. W. and Erwin D. H. (2016) Earth's oxygen cycle and the evolution of animal life. *Proc. Natl. Acad. Sci. U. S. A.* **113**, 8933–8938.

Reinhard C. T., Raiswell R., Scott C., An Bar A. D. and Lyons T. W. (2009) A late archean sulfidic sea stimulated by early oxidative weathering of the continents. *Science* **326**, 713–716.

Rolison J. M., Stirling C. H., Middag R. and Rijkenberg M. J. A. (2017) Uranium stable isotope fractionation in the Black Sea: Modern calibration of the $^{238}U/^{235}U$ paleo-redox proxy. *Geochim. Cosmochim. Acta* **203**, 69–88.

Scholz F., Baum M., Siebert C., Eroglu S., Dale A. W., Naumann M. and Sommer S. (2018) Sedimentary molybdenum cycling in the aftermath of seawater inflow to the intermittently euxinic Gotland Deep, Central Baltic Sea. *Chem. Geol.* **491**, 27–38.

Scholz F., Hensen C., Noffke A., Rohde A., Liebetrau V. and Wallmann K. (2011) Early diagenesis of redox-sensitive trace metals in the Peru upwelling area - response to ENSO-related oxygen fluctuations in the water column. *Geochim. Cosmochim. Acta* **75**, 7257–7276.

Scholz F., McManus J. and Sommer S. (2013) The manganese and iron shuttle in a modern euxinic basin and implications for molybdenum cycling at euxinic ocean margins. *Chem. Geol.* **355**, 56–68.

Scholz F., Severmann S., McManus J. and Hensen C. (2014) Beyond the Black Sea paradigm: The sedimentary fingerprint of an open-marine iron shuttle. *Geochim. Cosmochim. Acta* **127**, 368–380.

Scholz F., Siebert C., Dale A. W. and Frank M. (2017) Intense molybdenum accumulation in sediments underneath a nitrogenous water column and implications for the reconstruction of paleo-redox conditions based on molybdenum isotopes. *Geochim. Cosmochim. Acta* **213**, 400–417.

Schuth S., Brüske A., Hohl S. V., Jiang S. Y., Meinhardt A. K., Gregory D. D., Viehmann S. and Weyer S. (2019) Vanadium and its isotope composition of river water and seawater: Analytical improvement and implications for vanadium isotope fractionation. *Chem. Geol.* **528**, 119261.

Severmann S., Lyons T. W., Anbar A., McManus J. and Gordon G. (2008) Modern iron isotope perspective on the benthic iron shuttle and the redox evolution of ancient oceans. *Geology* **36**, 487–490.

Siebert C., McManus J., Bice A., Poulson R. and Berelson W. M. (2006) Molybdenum isotope signatures in continental margin marine sediments. *Earth Planet. Sci. Lett.* **241**, 723–733.

Siebert C., Nägler T. F., von Blanckenburg F. and Kramers J. D. (2003) Molybdenum isotope records as a potential new proxy for paleoceanography. *Earth Planet. Sci. Lett.* **211**, 159–171.

Spencer D. and Brewer P. (1971) on the Distribution of Manganese and Other Trace Metals Dissolved in Waters of the Black Sea. *J. Geophys. Res.* **76**, 5877–5892.

Sperling E. A., Halverson G. P., Knoll A. H., MacDonald F. A. and Johnston D. T. (2013) A basin redox transect at the dawn of animal life. *Earth Planet. Sci. Lett.* **371–372**, 143–155.

Tanaka M., Ariga D., Kashiwabara T. and Takahashi Y. (2018) Adsorption mechanism of molybdenum(VI) on manganese oxides causing a large isotope fractionation. *ACS Earth Sp. Chem.* **2**, 1187–1195.

Them T. R., Gill B. C., Caruthers A. H., Gerhardt A. M., Gröcke D. R., Lyons T. W., Marroquín S. M., Nielsen S. G., João P. T. A. and Owens J. D. (2018) Thallium isotopes reveal protracted anoxia during the Toarcian (Early Jurassic) associated with volcanism, carbon burial, and mass extinction. *Proc. Natl. Acad. Sci. U. S. A.* **115**, 6596–6601.

Vorlicek T. P., Helz G. R., Chappaz A., Vue P., Vezina A. and Hunter W. (2018) Molybdenum burial mechanism in sulfidic sediments: Iron-sulfide pathway. *ACS Earth Sp. Chem.* **2**, 565–576.

Wanty R. B. and Goldhaber M. B. (1992) Thermodynamics and kinects of reactions involving vanadium in natural systems: Accumulation of vanadium in sedimentary rocks. *Geochim. Cosmochim. Acta* **56**, 1471–1483. Available at: http://dx.doi.org/10.1016/0016-7037(92)90217-7.

Wasylenki L. E., Rolfe B. A., Weeks C. L., Spiro T. G. and Anbar A. D. (2008) Experimental investigation of the effects of temperature and ionic strength on Mo isotope fractionation during adsorption to manganese oxides. *Geochim. Cosmochim. Acta* **72**, 5997–6005.

Wasylenki L. E., Weeks C. L., Bargar J. R., Spiro T. G., Hein J. R. and Anbar A. D. (2011) The molecular mechanism of Mo isotope fractionation during adsorption to birnessite. *Geochim. Cosmochim. Acta* **75**, 5019–5031.

Wijsman J. W. M., Middelburg J. J. and Heip C. H. R. (2001) Reactive iron in Black Sea sediments: Implications for iron cycling. *Mar. Geol.* **172**, 167–180.

Wu F., Owens J. D., Huang T., Sarafian A., Huang K. F., Sen I. S., Horner T. J., Blusztajn J., Morton P. and Nielsen S. G. (2019a) Vanadium isotope composition of seawater. *Geochim. Cosmochim. Acta* **244**, 403–415.

Wu F., Owens J. D., Scholz F., Huang L., Li S., Riedinger N., Peterson L. C., German C. R. and Nielsen S. G. (2020) Sedimentary vanadium isotope signatures in low oxygen marine conditions. *Geochim. Cosmochim. Acta* **284**, 134–155.

Wu F., Owens J. D., Tang L., Dong Y. and Huang F. (2019b) Vanadium isotopic fractionation during the formation of marine ferromanganese crusts and nodules. *Geochim. Cosmochim. Acta* **265**, 371–385.

Wu F., Qi Y., Yu H., Tian S., Hou Z. and Huang F. (2016) Vanadium isotope measurement by MC-ICP-MS. *Chem. Geol.* **421**, 17–25.

Wu F., Qin T., Li X., Liu Y., Huang J. H., Wu Z. and Huang F. (2015) First-principles investigation of vanadium isotope fractionation in solution and during adsorption. *Earth Planet. Sci. Lett.* **426**, 216–224.

Xiao S. (2013) Oxygen and early animal evolution. In *Treatise on Geochemistry* (eds. H. D. Heinrich and K. K. Turekian), Second Edition. Elsevier, Oxford, pp. 231–250.

Yigiterhan O., Murray J. W. and Tugrul S. (2011) Trace metal composition of suspended particulate matter in the water column of the Black Sea. *Mar. Chem.* **126**, 207–228.

Associate editor: Susan Halsall Little